

Drosophila long-term memory formation involves regulation of cathepsin activity

Daniel Comas*, Florian Petit* & Thomas Preat

Développement, Évolution et Plasticité du Système Nerveux, CNRS, 1, Avenue de la Terrasse, 91190 Gif sur Yvette, France

*These authors contributed equally to this work.

Whereas short-term memory lasts from minutes to hours, long-term memory (LTM) can last for days or even an entire lifetime. LTM generally forms after spaced repeated training sessions and involves the regulation of gene expression^{1,2}, thereby implicating transcription factors in the initial steps of LTM establishment³. However, the direct participation of effector genes in memory formation has been rarely documented, and many of the mechanisms involved in LTM formation remain to be understood. Here we describe a *Drosophila melanogaster* mutant, *crammer* (*cer*), which shows a specific LTM defect. The *cer* gene encodes an inhibitor of a subfamily of cysteine proteinases, named cathepsins, some of which might be involved in human Alzheimer's disease⁴. The Cer peptide was found in the mushroom bodies (MBs), the *Drosophila* olfactory memory centre and in glial cells around the MBs. The overexpression of *cer* in glial cells but not in MB neurons induces a decrease in LTM, suggesting that Cer might have a role in glia and that the concentration of the Cer peptide is critical for LTM. In wild-type flies, *cer* expression transiently decreases after LTM conditioning, indicating that cysteine proteinases are activated early in LTM formation.

The MBs form a prominent bilateral structure of the insect brain. They are essential for short-term memory (STM), and many of the proteins involved in the early phases of memory establishment are preferentially expressed in the MBs or in neurons projecting to them⁵. We showed that MBs are also involved in LTM^{6,7}. Moreover, LTM mutants have been isolated recently⁸, but MB neuronal plasticity after LTM training remains to be characterized.

To acquire additional insights into LTM mechanisms, we have analysed *Drosophila* enhancer-trap Gal4 strains showing MB-specific expression. Flies were conditioned by exposure to an odour paired with electric shocks and subsequent exposure to a second odour in the absence of a shock. One of these strains, *MZ1180* (refs 9, 10), which we have named *crammer*^P (*cer*^P), displayed a decrease in 24-h LTM after spaced training, but a normal 24-h memory capacity after massed training, a conditioning

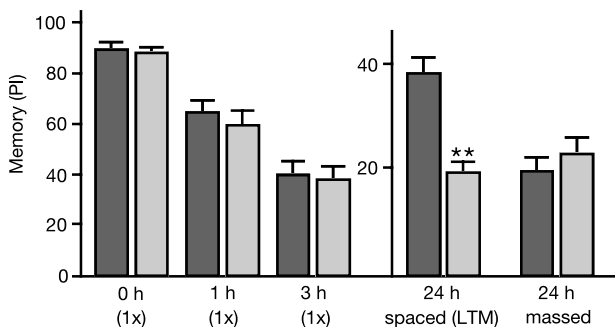


Figure 1 *cer*^P is a specific LTM mutant. Performance indices (PIs) were measured 1 and 3 h after a single conditioning cycle, and 24 h after spaced or massed training. Dark grey bars, CS; pale grey bars, *cer*^P. Results are means and s.e.m.; *n* = 8–10 groups. Asterisks indicate significant differences in a *t*-test (*P* < 0.01).

protocol that does not induce LTM² (Fig. 1). STM induced after a single training cycle was also normal, showing that *cer*^P is a specific LTM mutant. The LTM defect of *cer* is recessive (Supplementary Fig. 1). We performed excision experiments to generate revertant strains as well as additional mutant alleles. The excision line *cer*^{E29} displayed a specific LTM defect; in contrast, the *cer*^{E3} strain exhibited normal memory (Supplementary Fig. 1). Taken together, these results show that we have isolated a new LTM mutant with a P-element insertion.

Polymerase chain reaction (PCR) rescue experiments revealed that the P-element in *cer*^P flies was inserted 211 base pairs (bp) upstream of the gene encoding the succinyl-coenzyme A synthetase flavoprotein subunit (*Scs-fp*) and 53 bp downstream of the *CG10460* gene (Fig. 2a). Quantitative reverse transcriptase PCR (RT-PCR) (Fig. 2b) and northern blot (data not shown) analyses were performed to determine which gene was affected by the P-element insertion. Expression of *scs-fp* was normal in *cer*^P mutants, but expression of *CG10460* was strongly reduced, indicating that this gene corresponds to *cer* (Fig. 2b). Similar results were obtained by western blot analysis with a polyclonal antibody raised

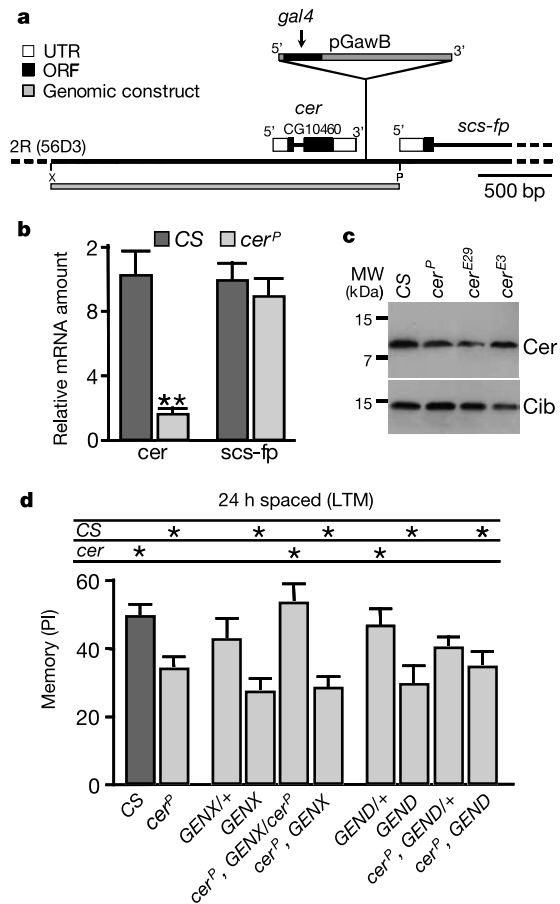


Figure 2 *cer* encodes a cathepsin inhibitor. **a**, The Gal4 P-element in *cer*^P flies is inserted between the *cer* and *scs-fp* genes. The genomic fragment used for the rescue experiment is shown with a grey bar. X, *Xba*I; P, *Pst*I; ORF, open reading frame; UTR, untranslated region. **b**, *cer* mRNA expression is affected by the P-element insertion, as measured by quantitative RT-PCR. Results are means and s.e.m.; *n* = 10–12 total RNA extractions. **c**, Similar results were obtained in a western blot assay. Densitometry analysis yielded Cer/Ciboulot (Cib) ratios of CS = 0.78 ± 0.24, *cer*^P = 0.37 ± 0.11, *cer*^{E3} = 1.29 ± 0.27 and *cer*^{E29} = 0.32 ± 0.05 (*n* = 5). **d**, The mutant phenotype can be rescued by the insertion of one genomic copy of the wild-type *cer*⁺ gene. The two upper lines represent significant differences between each score and the scores of CS or *cer*^P. PI, performance index. Results are means and s.e.m.; *n* = 6–10 groups. Asterisk indicates significant differences in a *t*-test (*P* < 0.05).

against Cer (Fig. 2c). As expected, a decreased level of Cer was found in the mutant excision *cer^{E29}*, and a normal level was found in the revertant excision *cer^{E3}* (Fig. 2c).

Sequence comparisons showed that Cer is highly similar to the amino-terminal regions of cathepsins L, a subfamily within the papain-like cysteine proteinase family (Supplementary Fig. 2a). Cysteine proteinases, which are generally synthesized as inactive proenzymes with an inhibitory N-terminal propeptide region, range in size from 300 to 350 amino acids. Interestingly, Cer is only 79 amino acids long (observed molecular mass 9.5 kDa), and it lacks the cysteine proteinase catalytic region, suggesting that it might act as a *trans*-inhibitor of cysteine proteinase(s)¹¹.

We performed experiments *in vitro* to assess the effect of Cer on the human liver cathepsins L and B and human papain. Cer was able to inhibit cathepsins L and B competitively ($K_i = 25$ nM and 30 nM, respectively; Supplementary Fig. 2b), but it could not inhibit papain even at 1 μ M (data not shown). These K_i values are similar to that described for other cathepsin inhibitors such as CTLA-2 β , a mammalian inhibitor of cathepsin L¹². Although the target(s) of Cer *in vivo* remain(s) to be identified, a *Drosophila* protein-protein interactions map has recently been generated showing that Cer interacts strongly with three proteins¹³ that are all cathepsins. Two of them correspond to cathepsin B group and seem to be expressed in the adult brain (as seen by northern blot assay; D.C., L. Zinck and

T.P., unpublished data). Those two cathepsins B constitutively lack the pro-inhibitor region. Cer is therefore probably needed to control their activity *in trans*.

To rescue the *cer^P* LTM phenotype, we introduced a genomic construction carrying the *cer⁺* gene with 1.5 kilobases (kb) of upstream sequence and 250 bp of downstream sequence (Fig. 2a). Rescue of the *cer^P* phenotype was observed in the presence of a single copy of the *cer⁺* transgene, indicating that this construct carries *cer* regulating sequences (Fig. 2d). In contrast, the presence of two copies of *cer⁺* could not rescue the *cer^P* LTM defect. Moreover, *cer⁺* flies expressing two additional genomic copies showed a decrease in LTM (Fig. 2d) but their STM remained normal (data not shown). Thus, *cer* overexpression affects LTM as severely as does a constitutive decrease in the concentration of *cer* mRNA. Taken together, these results show that the concentration of Cer must be within a short range of that in the wild type to form a normal LTM.

In which brain cells is *cer* specifically expressed? When the *cer Gal4* enhancer-trap line was crossed with the reporter strain *P(UAS-mCD8-GFP)*, MBs were found to be strongly labelled together with large cells (Fig. 3a). Unfortunately, our anti-Cer antibody was not able to detect the peptide on tissues. Therefore, to identify directly the sites at which *cer* is expressed, we inserted the green fluorescent protein (GFP) open reading frame before the *cer* stop codon in the previously described genomic construct (Fig. 2a). Because a fragment carrying the same genomic sequences could rescue the LTM *cer* phenotype, we postulated that this fusion protein would be expressed in cells required for normal Cer function. Expression was observed in the MBs, and γ lobes were more strongly labelled than α/β lobes (Fig. 3b). MB neuron cell bodies were not strongly labelled. In the cortex and in the neuropile, large cells expressing Cer-GFP were found around the MB calyces and near MB lobes. These cells, which were also detected in *cer^P/P(UAS-mCD8-GFP)* individuals, had no axonal projections, indicating that they might be glial cells. Indeed, they did not express the nuclear neuronal cell marker Elav (ref. 14) (data not shown). In contrast, some of these cells were found to express the nuclear glial cell marker Repo (Fig. 3c-e). Some *cer*-expressing cells seem Repo-negative and Elav-negative. Because Elav is expressed in all neurons¹⁴, whereas the anti-Repo antibody does not label all glial cells, the large Cer-expressing cells most probably correspond to glia. Cer is therefore expressed in both MB neurons and adjacent glial cells.

To further delimit the brain structures in which the concentration of Cer is critical for LTM formation, we overexpressed *cer* with the

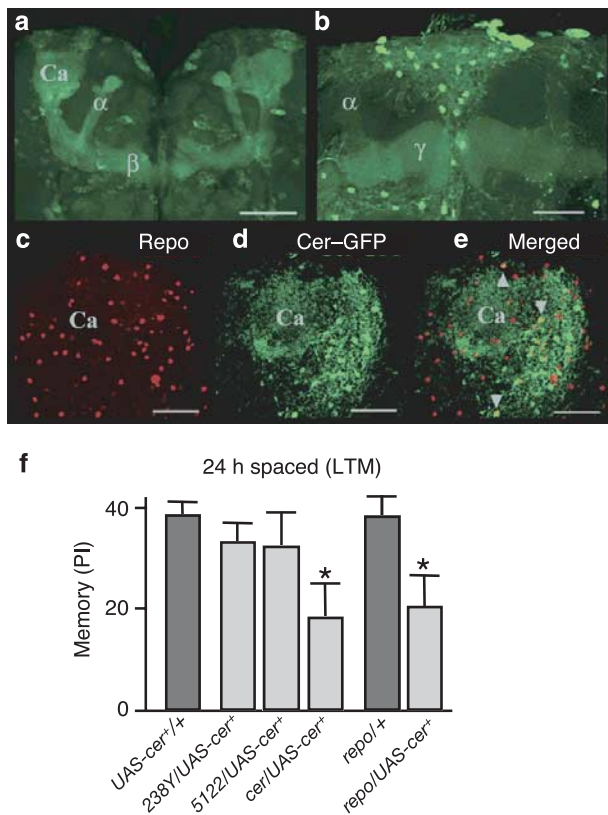


Figure 3 *cer* is expressed in MB neurons and in glial cells. **a**, Expression in a *cer^P-Gal4/P(UAS-mCD8-GFP)* line. **b**, Brain labelling of the 191 transgenic line carrying the Cer-GFP fusion protein, as viewed by confocal microscopy. **c**, A 191 brain stained with an antibody against Repo. **d**, Cer-GFP labelling. **e**, Colocalization of Cer-GFP and Repo. Regions of overlap are indicated by arrow heads. Scale bar, 40 μ m. **f**, Overexpression of *cer* with the *cer^P-Gal4* driver and with the glial driver *Repo-Gal4* induces an abnormal 24-h LTM. No effect was observed for overexpression in two different MB Gal4 lines, 238Y and 5122. Ca, calyx; α , alpha vertical lobe; β , beta medial lobe; γ , gamma medial lobe. PI, performance index. Results are means and s.e.m.; $n = 6-10$ groups. Asterisk indicates significant differences in a *t*-test ($P < 0.05$).

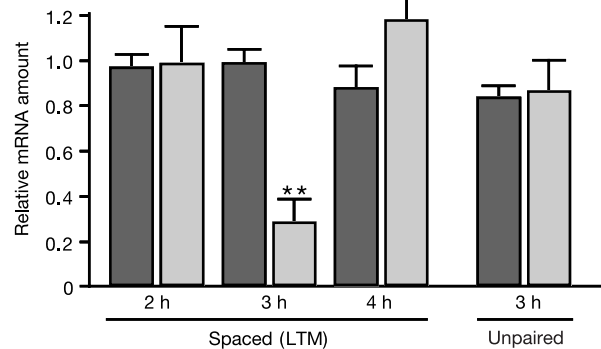


Figure 4 The level of *cer* mRNA is regulated after LTM conditioning. The level of *cer* mRNA is downregulated 3 h after LTM conditioning in the *CS* wild-type strain. An unpaired training does not affect the level of *cer* mRNA. Dark grey bars, untrained; pale grey bars, trained. Results are means and s.e.m. Asterisks indicate significant differences in a *t*-test ($P < 0.01$).

Gal4/UAS system. We observed a significant decrease in LTM conferred by the *cer-Gal4* driver (Fig. 3f), confirming the dosage effect found with the genomic insert. Interestingly, a similar LTM defect was observed when *cer* was overexpressed with the *repo-Gal4* glial-specific driver¹⁵. In contrast, no effect was seen when *cer* was overexpressed with the MB drivers 238Y (ref. 16) and 5122 (Fig. 3f) (the 5122 expression pattern is shown in Supplementary Fig. 3). These results indicate that the glial cells expressing *cer* might be involved in LTM formation. Indeed, neuron-like roles have recently been found for vertebrate glial cells. Some glial cells are able to integrate neuronal inputs, modulate synaptic activity, and process signals related to learning and memory¹⁷. *Cer* might be involved in the induction of neuronal plasticity by modulating crosstalk between neurons and glial cells.

Because the concentration of *Cer* seems to be a key factor in the establishment of LTM, we asked whether the *cer* transcript is regulated in the wild-type strain after LTM conditioning. We performed quantitative RT-PCR experiments at different time points after LTM training and found that the *cer* mRNA level decreased specifically 3 h after the end of training, in comparison with its level in untrained flies (Fig. 4). However, no significant change was observed 2 or 4 h after training (Fig. 4), indicating that the decrease in *cer* expression must occur in a narrow window of time to permit LTM formation. Similar results were obtained in western blot analysis: a 30% decrease in *Cer* level was observed between 3 and 4 h after conditioning (data not shown). Thus, the protein decay occurs slightly after the mRNA decay. Expression of *scs-fp* mRNA, the *cer*-adjacent gene, was not affected by LTM training (data not shown). Moreover, wild-type flies subjected to unpaired and repetitive odours and shocks, a regimen that does not induce learning, showed no variation in *cer* expression (Fig. 4). The sharp modulation of *cer* mRNA is therefore correlated with LTM formation.

What is the physiological meaning of the decrease in *cer* expression 3 h after LTM training? In the mouse, two waves of hippocampal mRNA synthesis are required for LTM formation after contextual fear conditioning¹⁸. Similar waves of gene expression have been described in *Hermisenda crassicornis* after associative conditioning¹⁹. Moreover, the simultaneous inhibition of multiple caspases (a family of cysteine proteinases) in the hippocampus blocks long-term, but not short-term, spatial memory²⁰. Our results extend these observations: we show that the expression of *cer*, which encodes an inhibitor of cysteine proteinases, is reduced for a short interval 3 h after training, thus probably leading to a transient activation of its cysteine proteinase(s) target(s). Significantly, prolonged cysteine proteinase activation is associated with neuronal degeneration in Alzheimer's disease: regions that contain maximal amounts of amyloid precursor protein also express maximal concentrations of cathepsin B and cathepsin L mRNA, indicating that the memory deficit of these patients might be linked to the deregulation of biochemical pathways involved in neuronal brain plasticity^{4,21}. We speculate that the memory deficit observed in flies with constitutively decreased concentrations of *Cer* might parallel this situation. □

Methods

Conditioning

The wild-type reference stock was *Canton-Special* (CS). The *cer^P* and all other strains used for memory experiments were outcrossed to flies of the CS background. Flies were conditioned by exposure to an odour paired with electric shocks and subsequent exposure to a second odour in the absence of shock, as described previously⁶.

Excisions and PCR rescue

Excision experiments were performed as described previously²². Genomic DNA adjacent to the P-element insertion was isolated by inverse PCR as described in <http://www.fruitfly.org/about/methods/inverse.pcr.html>.

Quantitative RT-PCR

Total RNA from the heads of conditioned or naive flies (1–2 µg) was used as a template for

reverse transcription using an oligo(dT) and SuperScript II reverse transcriptase (Invitrogen). Quantitative PCR was performed in accordance with the protocols provided with the LightCycler thermocycler (Roche) and the LightCycler – FastStart DNA Master SYBR Green I kit. The primers used were designed to amplify 60–80-bp fragments at the exon–intron boundary. Results were analysed in accordance with the instructions of the LightCycler software (version 3.5, Roche Molecular Biochemicals). The levels of *cer* and *scs-fp* mRNA were also normalized to the level of α -*Tub84B* mRNA.

Antibody production and western blot analysis

The *Cer*–glutathione S-transferase (*Cer*–GST) fusion protein was produced as described previously²³. Rabbits were injected dorsally several times every month for 3 months with 250 µg of the *Cer*–GST fusion protein mixed with Freund's adjuvant.

SDS–PAGE (with 70 µg of total adult head protein extract) and western blot analysis were performed as described previously²⁴. The membrane was incubated with polyclonal antiserum against the *Cer*–GST fusion protein (dilution 1:4,000) or with antiserum against Ciboulot (dilution 1:8,000), as described previously²³. The intensity of *Cer*-specific signals was normalized to that of Ciboulot-specific signals.

Cer inhibition assay

Cer activity was assayed as described for *Bombyx* cysteine proteinase inhibitor (BCPI) or CTLA-2 α (refs 12, 25), with a Safas flx spectrofluorimeter, *Cer* (0–200 nM), benzoyloxycarbonyl-Phe-Arg-7-amino-4-methylcoumarin as a substrate (3, 4.5 and 6 µM; Calbiochem, La Jolla, California), human liver cathepsin B and L (25 and 10 nM, respectively; Calbiochem) and papain (100 nM; Sigma, St Louis, Missouri).

Constructions

To create the genomic *cer⁺* construct the clone BACR21D20 was digested with *Pst*I and *Xba*I. A 2,296-bp fragment (carrying the *cer⁺* gene with 1.5 kb of sequence upstream of the transcription initiation site and 250 bp of downstream sequence) was cloned into pCaSpeR-4. Two transgenic lines, *GENX* and *GEND*, were obtained, with the P-element inserted in the second and third chromosome, respectively. Western blots were quantified and we observed that homozygous *GENX* and *GEND* had respectively twofold and threefold more *Cer* than CS (data not shown).

The *Cer*–GFP fusion protein construct was generated with the pCaSpeR-4 construction described above, by inserting GFP in phase before the *cer* stop codon. The *cer* 5' region until before the stop codon (*Bst*EII/*Bam*HI), the GFP open reading frame (*Bam*HI/*Xba*I) and the rest of *cer* (the 3' region from the stop codon and 250 bp of its downstream sequence (*Xba*I/*Pst*I) were amplified by PCR by using specific primers with the indicated restriction sites. All three PCR products were digested with appropriate restriction enzymes and the three products were cloned into *Bst*EII/*Pst*I-digested pCaSpeR-4 in a four-way ligation reaction.

To create the UAS-*cer⁺* construct a full-length *cer⁺* cDNA was isolated from the BDGP clone LP06209 and cloned into *Bgl*II/*Xba*I-digested pCaSpeR-UAS.

Immunohistochemical analysis

Drosophila brains were dissected as described previously⁶, then stained with the anti-Repo monoclonal antibody (dilution 1:100) or with the anti-Elav monoclonal antibody (dilution 1:10,000). Goat anti-mouse secondary antibody conjugated with Alexa-Fluor 568 (Interchim) was used at a dilution of 1:1,000. Expression was examined with a Leica (Wetzlar, Germany) TCS SP2 laser scanning confocal microscope.

Received 13 January; accepted 3 June 2004; doi:10.1038/nature02726.

- Bailey, C. H., Bartsch, D. & Kandel, E. R. Toward a molecular definition of long-term memory storage. *Proc. Natl Acad. Sci. USA* **93**, 13445–13452 (1996).
- Tully, T., Preat, T., Boynton, S. C. & Del Vecchio, M. Genetic dissection of consolidated memory in *Drosophila*. *Cell* **79**, 35–47 (1994).
- Alberini, C. M., Ghirardi, M., Metz, R. & Kandel, E. R. *C/EBP* is an immediate-early gene required for the consolidation of long-term facilitation in *Aplysia*. *Cell* **76**, 1099–1114 (1994).
- Callahan, L. M., Chow, N., Cheetham, J. E., Cox, C. & Coleman, P. D. Analysis of message expression in single neurons of Alzheimer's disease brain. *Neurobiol. Aging* **19**, S99–105 (1998).
- Waddell, S. & Quinn, W. G. Flies, genes, and learning. *Annu. Rev. Neurosci.* **24**, 1283–1309 (2001).
- Pascual, A. & Preat, T. Localization of long-term memory within the *Drosophila* mushroom body. *Science* **294**, 1115–1117 (2001).
- Isabel, G., Pascual, A. & Preat, T. Exclusive consolidated memory phases in *Drosophila*. *Science* **304**, 1024–1027 (2004).
- Dubnau, J. *et al.* The *staufen/pumilio* pathway is involved in *Drosophila* long-term memory. *Curr. Biol.* **13**, 286–296 (2003).
- Ito, K., Urban, J. & Technau, G. M. Distribution, classification and development of *Drosophila* glial cells in the late embryonic and early larval ventral nerve cord. *Wilhelm Roux Arch. Dev. Biol.* **204**, 284–307 (1995).
- Ito, K., Awano, W., Suzuki, K., Hiromi, Y. & Yamamoto, D. The *Drosophila* mushroom body is a quadruple structure of clonal units each of which contains a virtually identical set of neurons and glial cells. *Development* **124**, 761–771 (1997).
- Wiederanders, B. The function of propeptide domains of cysteine proteinases. *Adv. Exp. Med. Biol.* **477**, 261–270 (2000).
- Delaria, K. *et al.* Inhibition of cathepsin L-like cysteine proteases by cytotoxic T-lymphocyte antigen-2 beta. *J. Biol. Chem.* **269**, 25172–25177 (1994).
- Giot, L. *et al.* A protein interaction map of *Drosophila melanogaster*. *Science* **302**, 1727–1736 (2003).
- O'Neill, E. M., Rebay, L., Tjian, R. & Rubin, G. M. The activities of two *Ets*-related transcription factors required for *Drosophila* eye development are modulated by the Ras/MAPK pathway. *Cell* **78**, 137–147 (1994).
- Sepp, K. J., Schulte, J. & Auld, V. J. Peripheral glia direct axon guidance across the CNS/PNS transition zone. *Dev. Biol.* **238**, 47–63 (2001).

16. Armstrong, J. D., de Belle, J. S., Wang, Z. & Kaiser, K. Metamorphosis of the mushroom bodies; large-scale rearrangements of the neural substrates for associative learning and memory in *Drosophila*. *Learn. Mem.* **5**, 102–114 (1998).
17. Kurosinski, P. & Gotz, J. Glial cells under physiologic and pathologic conditions. *Arch. Neurol.* **59**, 1524–1528 (2002).
18. Igaz, L. M., Vianna, M. R., Medina, J. H. & Izquierdo, I. Two time periods of hippocampal mRNA synthesis are required for memory consolidation of fear-motivated learning. *J. Neurosci.* **22**, 6781–6789 (2002).
19. Epstein, H. T., Child, F. M., Kuzirian, A. M. & Alkon, D. L. Time windows for effects of protein synthesis inhibitors on Pavlovian conditioning in Hermessenda: behavioral aspects. *Neurobiol. Learn. Mem.* **79**, 127–131 (2003).
20. Dash, P. K., Blum, S. & Moore, A. N. Caspase activity plays an essential role in long-term memory. *Neuroreport* **11**, 2811–2816 (2000).
21. Maccioni, R. B., Munoz, J. P. & Barbeito, L. The molecular bases of Alzheimer's disease and other neurodegenerative disorders. *Arch. Med. Res.* **32**, 367–381 (2001).
22. Boquet, L., Hitier, R., Dumas, M., Chaminade, M. & Preat, T. Central brain postembryonic development in *Drosophila*: implication of genes expressed at the interhemispheric junction. *J. Neurobiol.* **42**, 33–48 (2000).
23. Boquet, L., Boujemaa, R., Carlier, M. F. & Preat, T. C. Cytoskeleton regulates actin assembly during *Drosophila* brain metamorphosis. *Cell* **102**, 797–808 (2000).
24. Comas, D., Piulachs, M. D. & Belles, X. Fast induction of vitellogenin gene expression by juvenile hormone III in the cockroach *Blattella germanica* (L.) (Dictyoptera, Blattellidae). *Insect Biochem. Mol. Biol.* **29**, 821–827 (1999).
25. Kurata, M. et al. *Bombyx* cysteine proteinase inhibitor (BCPI) homologous to propeptide regions of cysteine proteinases is a strong, selective inhibitor of cathepsin L-like cysteine proteinases. *J. Biochem. (Tokyo)* **130**, 857–863 (2001).

Supplementary Information accompanies the paper on www.nature.com/nature.

Acknowledgements We thank M.F. Carlier, M. Hertzog and P. Mehlen for advice with biochemistry experiments; S. Brown and C. Talbot for confocal microscopy expertise; and T. Aoki, G. Didelot, G. Isabel and A. Pascual for their comments on this manuscript. This study was supported by a Human Frontier Science Program grant. E.P. was supported by the Ministère de la Recherche and the Fondation des Treilles. D.C. was supported by the Association pour la Recherche sur le Cancer and the European Community Marie Curie Program.

Competing interests statement The authors declare that they have no competing financial interests.

Correspondence and requests for materials should be addressed to T.P. (preat@iaf.cnrs-gif.fr).

Transmission of cutaneous leishmaniasis by sand flies is enhanced by regurgitation of fPPG

Matthew E. Rogers¹, Thomas Ilg^{2*}, Andrei V. Nikolaev³, Michael A. J. Ferguson³ & Paul A. Bates¹

¹Liverpool School of Tropical Medicine, University of Liverpool, Pembroke Place, Liverpool L3 5QA, UK

²Max-Planck-Institut für Biologie, Abteilung Membranbiochemie, Corrensstrasse 38, 72076 Tübingen, Germany

³Division of Biological Chemistry and Molecular Microbiology, School of Life Sciences, The Wellcome Trust Biocentre, University of Dundee, Dundee DD1 5EH, UK

* Present address: Intervet Innovation GmbH, Zur Propstei, 55270 Schwabenheim, Germany

Sand flies are the exclusive vectors of the protozoan parasite *Leishmania*¹, but the mechanism of transmission by fly bite has not been determined nor incorporated into experimental models of infection. In sand flies with mature *Leishmania* infections the anterior midgut is blocked by a gel of parasite origin, the promastigote secretory gel^{2,3}. Here we analyse the inocula from *Leishmania mexicana*-infected *Lutzomyia longipalpis* sand flies. Analysis revealed the size of the infectious dose, the underlying mechanism of parasite delivery by regurgitation, and the novel contribution made to infection by filamentous proteophosphoglycan (fPPG), a component of promastigote secretory gel found

to accompany the parasites during transmission. Collectively these results have important implications for understanding the relationship between the parasite and its vector, the pathology of cutaneous leishmaniasis in humans and also the development of effective vaccines and drugs. These findings emphasize that to fully understand transmission of vector-borne diseases the interaction between the parasite, its vector and the mammalian host must be considered together.

Leishmaniasis is a parasitic disease that now infects some 12 million people worldwide, causing severe morbidity and mortality⁴. Infection is initiated by distinct life cycle stages, metacyclic promastigotes, that are introduced into the skin by fly bite along with sand fly saliva^{5–7}. *Leishmania* are known to express various 'virulence factors' in the sand fly, which may facilitate transmission to, and infection of, the mammalian host^{8–12}. However, despite these discoveries our knowledge of parasite molecules that facilitate sand fly transmission is still limited. Furthermore, a number of key issues of transmission remain unresolved, such as the true infective dose, the mechanism of parasite delivery and the biological consequences of these upon infection. Importantly, in all *Leishmania*-vector combinations examined so far, a gel-like plug—the parasite-derived promastigote secretory gel (PSG)—blocks the anterior parts of the midgut coincident with the accumulation of metacyclic promastigotes^{2,3}. An important structural component of PSG is filamentous proteophosphoglycan (fPPG), an unusual mucin-like glycoprotein unique to *Leishmania*^{13,14}. Here we address these issues regarding transmission and reveal a novel contribution made by *L. mexicana* PSG to the infection process.

To begin to understand the nature of the infective inoculum, we determined the number and composition of *L. mexicana* parasites delivered during transmission (see Methods). We adapted a membrane feeding system to collect parasites egested by infected sand flies, revealing an average of 1,086 parasites delivered per bite, highly enriched in metacyclic promastigotes (86–98%) (Table 1). The only previous investigations quantifying egested parasites have been made using microcapillary forced feeding^{15,16}. When this method was employed on *L. mexicana*-infected sand flies an average of 105 promastigotes was collected per sand fly ($n = 19$), significantly ($P < 0.005$) underestimating the size of the average infective dose egested under voluntary feeding conditions. To address the origin of the average 10^3 parasites delivered during transmission, we quantified the foregut populations in sand flies. The average foregut population in pre-fed flies was 118 promastigotes ($n = 10$), and in post-fed flies was 53 promastigotes ($n = 13$) per sand fly. These populations are considerably smaller than the number of promastigotes that were actually egested. Therefore, the main source of egested parasites (>90%) lies behind the pharynx, thus clearly demonstrating active regurgitation of parasites from the oesophagus and behind, and not merely inoculation of the foregut population.

Next we investigated the efficiency of sand fly transmission by comparing infections caused by a single fly bite with those generated by a syringe inoculation. From the above results, a syringe inoculum of 10^3 metacyclic promastigotes was used to simulate natural transmission, and BALB/c and CBA/Ca mice expressed non-healing and healing phenotypes, respectively (Fig. 1a, b). However, when individual mice were infected by single fly bites different outcomes were quantitatively (BALB/c) and qualitatively (CBA/Ca) observed. BALB/c mice exhibited greatly accelerated lesion development, these appearing four to five weeks earlier than syringe inoculation and rapidly increasing in size without healing (Fig. 1a), whereas CBA/Ca mice developed non-healing chronic lesions (Fig. 1b). By analysing *Leishmania* infection using single fly bites we provide definitive evidence that delivery by sand flies makes a contribution to *Leishmania* infection beyond simple injection of parasites.

One plausible explanation for the results described above is that sand flies egest 'exacerbation factors' along with metacyclic pro-